Soft Matter

Cite this: *Soft Matter*, 2012, **8**, 2792

www.rsc.org/softmatter

PAPER

Diffusive behaviour of PLL–PEG coated colloids on λ-DNA brushes – tuning hydrophobicity

Taiki Yanagishima,[a] Lorenzo Di Michele,[a] Jurij Kotar[a] and Erika Eiser[ab]

Received 9th February 2012, Accepted 3rd May 2012
DOI: 10.1039/c2sm25296a

We find 'sticky' 2D diffusion of poly-L-lysine–polyethylene glycol (PLL–PEG) coated silica colloids sedimented onto a brush of long, double stranded λ-DNA. The interaction is hypothesised to be hydrophobic, due to known physical properties of single and double stranded DNA and the systematic elimination of other known forces. The colloids are found to have variable affinity to the surface when prepared at different pH, even when the electrostatic environment of the brush is kept identical. Varied diffusive behaviour is observed: the diffusivity increases when the incubation pH is higher, and fewer beads are stuck to the brush surface. This sensitivity is found to agree with a simple model for the adsorption conditions of the PLL on the silica spheres. The significance of hydrophobicity is confirmed by capping the ssDNA 'sticky' end of the DNA, leading to a drastic enhancement of diffusivity of the particles on the brush.

1 Introduction

Surface control is crucial for the proper functioning of many modern biomedical devices. For instance, DNA biosensors and phage display technologies rely on specific affinity to a substrate. The sensitivity of such devices is reduced by non-specific interactions. Hence, there is a great need to have simple, reproducible techniques to control non-specific interactions. In the present paper, we describe a simple method to vary the strength of non-specific interactions of colloidal particles with a DNA-functionalized substrate.

There is a wide variety of (bio)physical systems where the interaction of surfaces with DNA plays a key role. Examples include DNA packaging,[1–3] translocation of DNA through pores[4–7] and DNA-mediated colloidal self-assembly.[8–15] Further to hybridisation, the basic physico-chemical properties of DNA give it features that are independent of Watson–Crick pairing, such as its elastic response[16–19] and hydrophobicity.[20–22] These affect not only the energetics of relevant processes, but also the dynamics that is determined by the interaction of the diffusing entity with its environment.

The temperature dependence of the strength of DNA hybridisation leads to a high temperature sensitivity of the 'stickiness' between colloidal particles and surfaces that have been functionalised with complementary DNA strands.[23] However, as we discuss below, non-specific interactions may also result in interactions between colloidal particles and surfaces. Here, we study the degree of "stickiness" between colloids coated with poly(L)lysine–polyethylene glycol (PLL–PEG) and solid surfaces coated with thick polyelectrolyte brushes composed of λ-DNA. The key point to note is that, although we use a DNA brush as a substrate to mimic DNA-functionalised materials, we use DNA that does *not* interact specifically with the colloidal particles. Hence the substrate–colloid interactions are purely electrostatic and/or hydrophobic. Importantly, we find that the affinity between the colloids and the DNA brush can be controlled by varying the pH during the functionalization of the colloids. As we study systems under conditions where the electrostatic interactions are strongly screened, we hypothesise that the colloid–substrate adhesion is largely due to the hydrophobicity of the DNA strands.[24] In particular, we show that beads incubated in different pH conditions within the physiological range, 7–9, display drastically different dynamic behaviour on the DNA brush. This pH dependence is potentially important because at present, colloids are usually functionalised at a pH value that is set by the most commonly used buffers (*e.g.* pH 7.2, standard pH of PBS). The present study suggests that a careful choice of the pH during colloidal incubation is crucial to control the degree of non-specific colloid–substrate interactions. Also, given an understanding of the underlying phenomenon, one can extend the framework of such a system to physically similar, non-DNA systems of grafted colloids undergoing diffusion on coated surfaces.[25]

In our study we used a combination of different experimental methods to trace the dynamics of the colloids, probe their surface charge and measure the thickness of the DNA brush. Specifically, to study the dynamics of the colloids we used video particle-tracking to determine the mean-squared displacements

[a]*Biological and Soft Systems Sector, Cavendish Laboratory, JJ Thomson Ave, Cambridge, CB3 0HE, UK. E-mail: ee247@cam.ac.uk; Fax: +44 (0)1223-337000; Tel: +44 (0)1223-337007*
[b]*BP Institute, Bullard Laboratories, Madingley Rd, CB3 0EZ Cambridge, UK. E-mail: ee247@cam.ac.uk; Fax: +44 (0)1223-765700; Tel: +44 (0) 1223-765701*

of the colloidal particles and thus calculate their diffusivity D. We quantify the degree of horizontal confinement by relating the horizontal mean-squared displacement of the colloids to an effective harmonic spring constant κ. To characterise the surface state of the PLL–PEG coated microspheres prepared under different conditions, we used zeta-potential measurements. Finally, we used confocal microscopy to characterise the thickness of the brush. To this end, we used an intercalating dye that allowed us obtain a three-dimensional reconstruction from stacks of confocal microscopy images.

2 Materials and methods

2.1 Glass cleaning and PLL–PEG absorption

The PLL–PEG used has a bottle-like structure consisting of a positively charged polylysine backbone with PEG side chains. The particular co-polymer used in these experiments was PLL (20 kDa)-*g*(3.5)-PEG (2 kDa), where the PLL-backbone had a molecular weight of 20 kDa, and each PEG side chain had a molecular weight of 2 kDa. The grafting ratio was 3.5, *i.e.* there is one PEG chain grafted every 3.5 lysines along the backbone, on average (Fig. 1).

In order to adsorb PLL–PEG evenly onto glass, the silica surface needs to be free of contaminants. Glass surfaces were soaked in 10% Hellmanex (Hellma, UK) solution for over 24 hours and rinsed in an excess of doubly distilled H_2O (ddH_2O). The surfaces for DNA grafting were, for the most part, 400 µl wells on 96 well plates with a number 1.5 coverslip thickness optical bottom (Nunc, US). 1.16 µm diameter silica microspheres (Microparticles Gmbh, Germany) were confirmed to be free of defects through imaging using an environmental scanning electron microscope (FEI Philips XL30 FEG ESEM), hence were used directly.

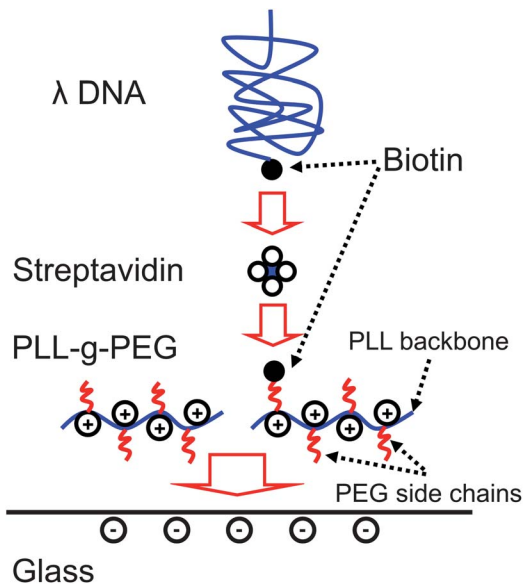

Fig. 1 Grafting scheme for λ-DNA to the surface following a 3-step procedure: (1) PLL–PEG is electrostatically adsorbed to the surface (2) streptavidin is bound to the surface *via* a biotin–avidin linkage. (3) Pre-biotinylated λ-DNA is added and bound to one of the open sites on the streptavidin.

Once the surfaces were prepared, the slides or microspheres were exposed to 0.5 mg ml^{-1} PLL–PEG or PLL–PEG–biotin (see Section 2.3) (Surface SolutionS Gmbh, Switzerland) (or PLL–PEG–biotin for DNA coating) in a 100 mM tris(hydroxymethyl) aminomethane (TRIS) buffer of chosen pH. Incubation was carried out overnight, to ensure homogeneous coverage. After coating, the wells were thoroughly rinsed with ddH_2O, while colloid solutions are centrifuged at 15 000 × *g* for two minutes to pellet the silica beads. The supernatant was removed, and the beads were resuspended in 100 mM TRIS buffer. The washing procedure was repeated three times.

2.2 λ-DNA biotinylation

λ-DNA has a double stranded ring structure that opens up when heated, revealing two short single-stranded ends with 12 base-pair complementary sequences. These are known as *cos1* and *cos2*.[26] Knowing the precise sequences,[27] we selectively functionalised one end with a biotinylated complementary strand and repaired the nick in the backbone using a ligase: following a modified protocol by Geerts *et al.*,[28] we first mixed 10 µl of an aqueous solution of λ-DNA (500 ng μl^{-1}) with 100 µl of 100 mM TRIS solution at pH 8. This high buffer concentration is maintained to aid the stability of the double strand. This was combined with 2 µl of a 50 µM aqueous custom *cos1*–biotin complex (Invitrogen) and incubated at 65 °C for 30 minutes, and allowed to cool slowly overnight. The nick in the dsDNA was repaired using T4 ligase (New England Biolabs) with an accompanying 10× buffer containing ATP – 3 µl of the ligase and 30 µl of the buffer is added to the tube, and allowed to react on a 20 RPM rotor for 2 hours. We inactivated the ligase by heating the solution at 65 °C for around 15 minutes. The ATP and unreacted oligos were separated out with a cellulose-membrane centrifugal filter (Vivacon 500 100k MWCO, Sartorius Stedim, UK), using 3 × 30 min cycles at 2500 RPM. On every cycle, the buffer was replaced with a sterile TRIS-EDTA buffer.

2.3 DNA grafting to surface and staining

The biotinylated λ-DNA was grafted to the surface using a streptavidin linker that attaches it to the PLL–PEG–biotin layer. A schematic is given in Fig. 1. 5 µl of 5 µg μl^{-1} aqueous solution of salt-free streptavidin from *Streptomyces avidinii* (Sigma Aldrich) was added along with 50 µl of 100 mM TRIS at pH 8, and left to incubate for 30 minutes. The biotinylated λ-DNA solution at approximately 50 ng μl^{-1} was then added and allowed to incubate overnight. ddH_2O rinses (×3) were carried out between each step.

The thickness and integrity of the DNA-brush were then verified with confocal-microscopy. To that end, the double-stranded DNA was stained with the intercalating dye SYTO 9 (Invitrogen, UK): 50 nM of dye was introduced and incubated for over 30 minutes, in agreement with suggested values by manufacturers for staining DNA microarrays. The layer was then flushed with ddH_2O and replenished with the appropriate buffer.

2.4 ζ Potential

The ζ potential of the colloids was measured using a Malvern Zetasizer ZS (Malvern, UK). The measured ζ potentials were

interpreted as a direct measure of the effective total surface charge density.

2.5 Microscopy and particle tracking

Bright-field microscopy (Eclipse Ti, Nikon, Japan) was used to visualise colloidal diffusion. A CCD camera (Stingray, Allied Visual Technologies) with a frame rate of approximately 100 Hz was used for video capture. For particle tracking we employed a method developed by Crocker and Grier[29] and implemented into an adapted MATLAB routine by Blair and Dufresne (http://physics.georgetown.edu/matlab/). We considered only trajectories of particles that were at least 10 colloidal diameters removed from any other colloidal particle, thus minimizing the effect of unwanted colloid–colloid interactions.

Confocal microscopy of a fluorescently stained DNA layer was achieved using a Leica CTR500 unit. Images were thresholded to include only fluorophore sites confined to the DNA layer by manual handling in ImageJ,[30] and their coordinates were reconstructed in MATLAB.

3 Results and discussion

3.1 Zeta potential measurements

First we measured the zeta potential of bare silica microspheres – results are given in Fig. 2. Five different pH conditions were used (7 to 9 in 0.5 steps) in 100 mM TRIS solution. Colloid concentrations were maintained at 0.005 vol% and sonicated for 15 minutes beforehand, to allow for a good transmission signal and to keep the colloids from aggregating, as the latter will influence the mobility. Readings were taken three times. The distribution of zeta potentials was confirmed to have one peak only, and the peak value was recorded. The error bars in Fig. 2 indicate the deviation of these peak values – the distribution width is discussed later.

From Fig. 2 it is evident that the surface becomes more strongly charged at higher pH. As the pH is raised, H^+ ions are depleted from the bulk and are also taken from the silanol groups on the silica, increasing the negative charge. Ion exchange occurs on significantly smaller length scales than the curvature of the microspheres. Saengsawang *et al.*[31] give the distance between charged sites as either 0.386 nm or 0.575 nm, depending on the

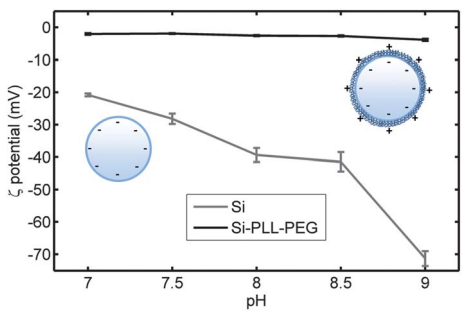

Fig. 2 Zeta potentials of bare silica particles and those coated with PLL–PEG in 100 mM TRIS at pH 7 to 9. The surface becomes more strongly charged at higher pH for the bare silica, while an approximate charge cancellation is seen in the PLL–PEG coated ones.

configuration, hence it is safe to assume that these values apply to flat silica surfaces, such as a coverslip.

Subsequently, PLL–PEG coated beads were measured (see also Fig. 2). These show a significantly reduced surface potential, as electrostatic adsorption of the PLL–PEG chains creates a composite surface with a reduced net charge. Given the high adsorption energy, the PEG side chains are forced to point into the bulk solution around the bead, creating a sterically stabilising layer. It is assumed that the polylysine is immobilised onto the surface, and is not affected by the external electric field of the Zetasizer.

It can be seen that the bare colloidal charge is roughly canceled by the adsorption of PLL–PEG. This is expected as, despite the polymeric nature of the PLL, there is no other interaction apart from Coulomb forces that bring it to the surface. Thus, it is clear that a higher silica surface charge directly corresponds to more PLL–PEG on the surface.

Two further points need to be considered: (1) though this is not reflected in Fig. 2, the width of the distributions is found to be significantly larger for low zeta potentials, at approximately ±5 mV. Low surface charge means low mobility, due to slow electrophoretic drift in the same field. The majority of the signal is thus made up of beads at the extremities of coating/non-coating, resulting in a lower peak at, say zero mV, and greater at higher values, resulting in a flattening of the distribution curve, hence, explaining the larger deviation. (2) There are reports of stability over a period of 3 weeks[32] in the presence of the same buffer. However, when the buffer pH is changed, we found that the same charge cancellation rule is found, with no overcharging phenomena. This implies that a more densely coated bead releases the polylysine once the surface charge changes.

3.2 DNA brush characterisation

The configuration of the DNA brushes is primarily determined by our grafting method, which simply allows free polymers to graft to the surface *via* biotin–avidin binding. Once a grafted monolayer in mushroom configuration has formed, further grafting becomes kinetically hindered.[33] Thus, it would be reasonable to think that the monolayer will either be in a mushroom regime, or at the boundary to an extended brush-regime. Given the extreme length of λ-DNA, it is in a quasi-neutral state, with blobs interacting in a self-avoiding manner, where the blob size is determined chiefly by electrostatics and Manning condensation.[34] Note that only monovalent buffers are used here, as it is not desirable to induce brush collapse.[35]

Given such a description, the thickness of the layer should be approximately the radius of gyration of the DNA layer ($R_g \approx$ 800 nm in a good solvent[11]), or slightly larger. A λ-DNA layer in pH 8, 100 mM TRIS was stained with SYTO-9 and imaged using confocal microscopy. Taking a stack of images through the DNA-layer and reconstructing local fluorescence maxima to a three-dimensional picture gave us an indication of the grafted layer thickness (Fig. 3): we observe a relatively sharp plateau region of 1.5–2 μm in thickness, slightly larger than $2R_g$ but significantly less than the contour length of λ-DNA, $L \approx$ 15 μm. Therefore we will refer to the DNA monolayer as a brush.

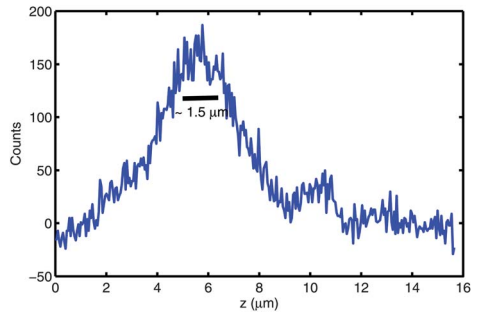

Fig. 3 Distribution of fluorophores over different z positions. The plateau of around 1.5 μm width indicates the thickness of the brush.

3.3 Particle trajectory analysis

3.3.1 Bare beads on λ-DNA. First, we examined the diffusive behavior of bare silica beads on the DNA-brush. We allowed the colloids to sediment onto the DNA brushes in 100 mM TRIS buffer. Because of the high density of silica, all the 1.15 μm large beads sedimented within 10 minutes, having a gravitational distribution of only a few μm in z-direction. For all pH values observed (7–9), the beads were almost immediately immobilised on contact with the DNA-brush, despite the negative charge on both the bead surfaces and the brush. This is most likely due to the strong hydrophobic interaction between bare, unstabilised silica surfaces and DNA. This concurs with the work of Liu *et al.*,[22] who observed adsorption of λ-DNA onto flat glass surfaces. They report an increased adsorption for surfaces that have not been deep-cleaned using harsh basic agents – this situation corresponds to the state of the microspheres we used.

3.3.2 PLL–PEG coated colloids on λ-DNA. Similar to the bare-bead experiments, we prepared dilute solutions of silica colloids sterically stabilised with PLL–PEG. 5 wells were prepared using identical procedures establishing the DNA-brush layers. Once the brushes were established the pH in each was changed to obtain 5 different pH conditions before the PLL–PEG beads were introduced. We immediately observed an increased mobility for all the beads, which we ascribed to the presence of the hydrophilic PEG layer on the surfaces.

In order to discern the effects of pH on the bead–brush interactions, independent of the ionic strength of the solvent, NaCl is added in the correct quantities. Thus we ensured the ionic strength to be 100 mM at all pHs. This ionic strength was chosen such that the PEG monolayer was behaving according to good solvent conditions. The radius of gyration of the PEG side-chains in solution R_g was found using an empirical equation given by Devanand and Selser,[36]

$$R_g = 0.215 M_w^{0.583\pm0.031}. \quad (1)$$

This equation is given in units of Ångstrom, and M_w is the average molecular weight. For PEG 2000, $R_g = 1.8$ nm. This is compared with the Debye screening length in a 100 mM salt buffer, given by $\lambda_D = (\varepsilon_r\varepsilon_0 k_B T/\sum_i^N n_i q_i^2)^{0.5}$, where ε_r and ε_0 are the relative and free space permittivities of the medium (in this case, water), $k_B T$ is the thermal energy and n_i and q_i are the number densities and charge of the N ionised species in solution. This gives $\lambda_D = 0.9$ nm, which is less than the radius of gyration of the PEG.

Summarising: the colloid–substrate affinity for this system is determined by the interaction between the DNA brush and a combination of either (a) the PEG or (b) the silica of the beads, when directly in contact (Fig. 4B). We know, from the bare bead experiments that latter is a strong, hydrophobic adsorption.

To determine diffusivities, we analysed the colloidal trajectories $x(t)$ for time intervals up to a few seconds in length. The diffusion coefficients were obtained from the time dependence of the mean-squared displacements (MSDs) of the colloids. Different methods are used to estimate the short-time diffusion constant of a particle, depending on whether it is trapped or diffusing freely. For particles that are freely diffusing in a plane parallel to the surface, we use $\langle x(t)^2\rangle = 4Dt$. For particles that undergo locally Brownian motion but that are trapped, we use the expression for the time dependence of the mean-squared displacement of a particle diffusing in a harmonic potential with spring constant κ.[37] The value of κ was determined from the plateau value of the mean-squared displacement:

$$\kappa = \frac{4k_B T}{\langle x^2\rangle_{plateau}}$$

Combining these with the relaxation in a harmonic potential, one gets the expression

$$\left\langle x(t)^2\right\rangle = \frac{4k_B T}{\kappa}\left(1 - \exp^{-\frac{D\kappa t}{k_B T}}\right). \quad (2)$$

Instrumental drift was accounted for by using a moving average high pass filter with a window of at least twice the maximum lag.

As can be seen from Fig. 4, the diffusion constant of colloidal particles on the soft substrate depends strongly on the pH at which the particles were functionalised. The more PLL–PEG is adsorbed to the colloidal surface, the higher their diffusivity and the weaker their confinement. The (gradual) transition from high to low diffusivity is centered around pH 8. The peak at high κ in the histograms for pH =7 and 7.5 indicates a lower bound: the true value of κ cannot be resolved, but may be higher than indicated.

3.3.3 Discussion of pH effect. We now describe the possible physical effects behind the strong change in diffusivity with the pH during the coating of colloids. It seems plausible that the low diffusivity for pH < 8 is due to the incomplete PLL–PEG coverage of the negatively charged surface of the silica beads. In that case there are too few negative charges to bind enough positively charged PLL chains to cover the whole microsphere surface.

For the PLL–PEG used, there are 3.5 lysine residues per PEG side chain (see Fig. 5A). These residues are assumed to be fully dissociated (one positively charged amine moiety per lysine residue). The charged units are distributed over an area determined by the Debye length λ_D and the radius of gyration of the PEG (approximately 1.8 nm), as there is a free energy penalty for overlapping adjacent strands. This short, $2 \times R_g$ long section of

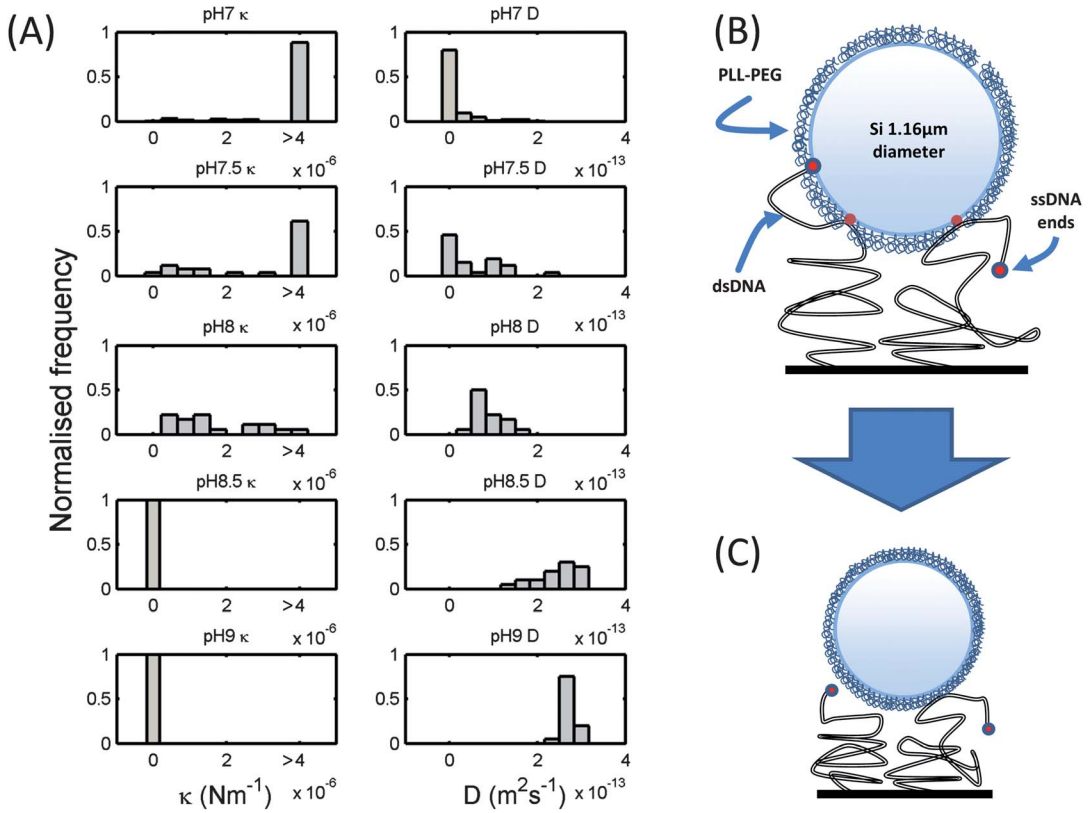

Fig. 4 (A) Short time diffusion constants D and confinement values κ for PLL–PEG coated beads on DNA surfaces in 100 mM TRIS, adjusted to 100 mM ionic strength using NaCl. Beads incubated at higher pH are more mobile, while those at lower pH have a higher affinity to the surface. There is a clear transition in the nature of the particles, from (B) DNA adhesion to the silica surface through small gaps on the surface to (C) a complete PEG coverage, allowing free diffusion. Note that strict histogram conventions are not observed at the extremities of the axes, to preserve the scale.

PLL and its 3.5 positive charges can interact with negative charges on the silica over an area determined by $\sim R_g \times \lambda_D$ – this equates to a charge density of $\sigma_{PLL} \approx 0.17$ C m^{-2}. Our measurements of the ζ potential values provides direct evidence for a pH dependence of the degree of charge cancellation. Then, the conclusion is that, in order to obtain full steric stabilisation, the pH needs to be such that the charge of the silica surface matches that of a PLL–PEG layer which fully covers the

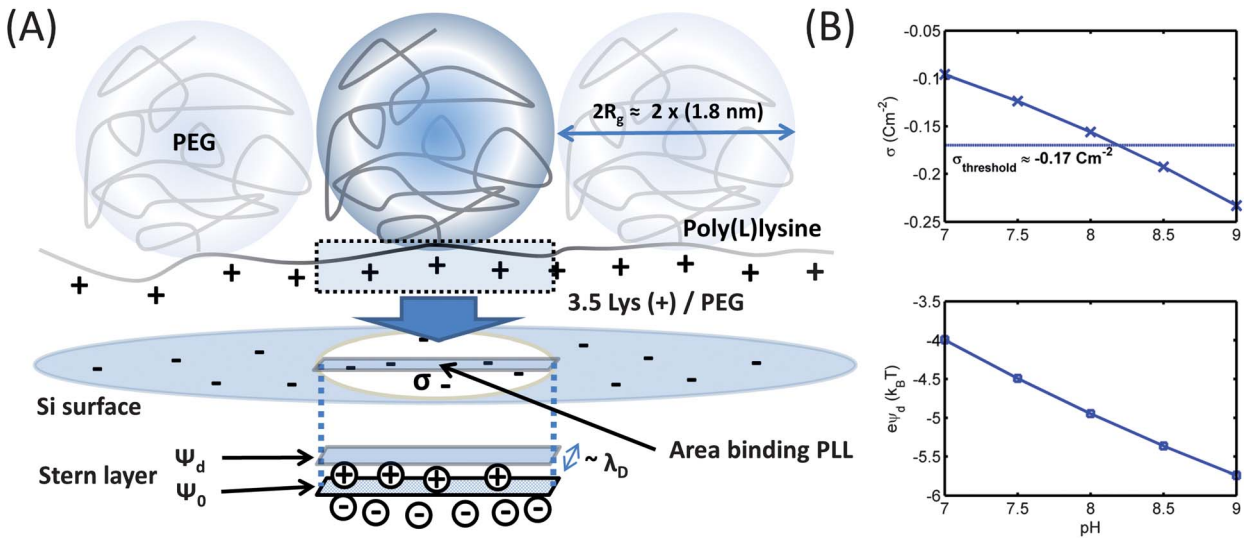

Fig. 5 (A) Diagram of PLL–PEG adsorption. PLL adsorbs onto a silica surface with charge density σ, characterised by surface potentials ψ_0 at the surface and ψ_d at the end of the Stern layer. (B) σ and adsorption energy $e\psi_d$ for different pH. The threshold charge density $\sigma_{threshold} \approx 0.17$ C m^{-2} is reached when the pH reaches 8. This agrees with the behaviour transition seen for particle dynamics.

colloidal surface. Substituting, this silica surface charge density threshold σ_{thr} is given by $\sigma_{thr} = \sigma_{PLL} \approx 0.17$ C m^{-2}.

The charge density of the surface σ is determined by two factors: (1) the surface charge can be found as a function of the electrostatic potential at the surface ψ_0 and the pK_a. ψ_0 is related to the diffuse layer potential ψ_d, the distance from the surface at which ions regain their mobility, by the capacitance of the silica–water interface[38] $C = 2.9$ F m^{-2}. (2) ψ_d can be found as a function of σ for a sufficiently flat surface and Debye length λ_D assuming flat double layers. The binding energy of the PLL can then be approximated by $e\psi_d$, where e is the elementary charge. The two relations are expressed as[39]

$$\psi_d(\sigma) = \frac{1}{\beta e}\ln\frac{-\sigma}{e\Lambda+\sigma} - (\mathrm{pH}-\mathrm{p}K)\frac{\ln(10)}{\beta e} - \frac{\sigma}{C} \quad (3)$$

$$\sigma(\psi_d) = \frac{2\varepsilon\varepsilon_0\lambda_D}{\beta e}\sinh\left(\frac{\beta e\psi_d}{2}\right), \quad (4)$$

where ε and ε_0 give relative and free space permittivities, β is the reciprocal of the thermal energy k_BT and $\Lambda = 8$ nm^{-2} is the number of available sites per area that can be charged on the silica surface. We found self-consistent values of σ and ψ_d for different pH conditions, given in Fig. 5B, using a pK_a value of 5.8.[40]

We find that the surface reaches $\sigma_{threshold}$ at the pH when we see a transition in behaviour between tethered motion and free diffusion. This is in agreement with our hypothesis, that the adhesivity of the surface is determined by the degree of coverage of the microspheres with PLL–PEG. Note also the high adsorption energies – this validates the long term stability of the layer.

It should be noted that this perfect agreement may be fortuitous, due to the choice of the width of the area with which the PLL chain interacts. Indeed, the electrostatic potential extends further than half a Debye length either side. However, it should be noted that the distance at which the potential drops to k_BT is probably too long a choice, as a k_BT binding energy is too low for stable adsorption. In fact, this lends credence to the converse argument that, given the good agreement with experimental data, the adsorption energy is just adequate for stable binding at a distance half λ_D from the chain. A more accurate calculation would need to account for the charge redistribution as a positive polyelectrolyte approaches the surface, but this is beyond the scope of this work.

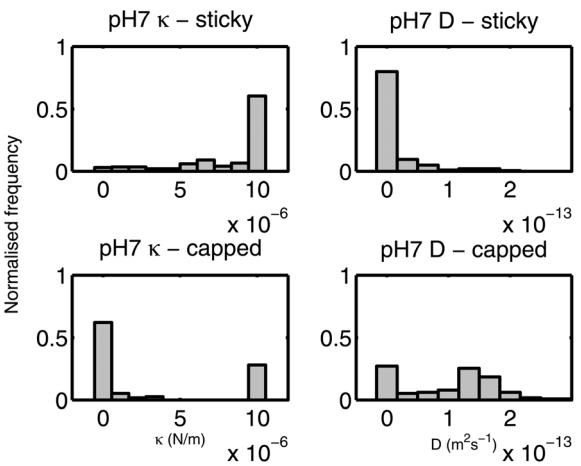

Fig. 6 A comparison of diffusivity D and confinement κ distributions for λ-DNA brushes with (sticky) and without (capped) a ssDNA end at pH 7.5. There is a clear increase in diffusivity when the ssDNA ends are capped, indicating that a large part of the bead–DNA interaction is hydrophobic.

3.3.4 Role of the ssDNA end. We still need to understand the adhesive interaction between the bare silica surface and the DNA brush. As discussed below, we can attribute this adhesion to hydrophobicity. Evidence for this hypothesis comes from a study where we modify the hydrophobicity of the λ-DNA brush by capping the short ssDNA 'sticky' group at the end of the strand: ssDNA is much more hydrophobic than dsDNA due to exposure of its bases. Interestingly, we find that capping the ssDNA sticky end groups has a large effect on the colloidal diffusivity.

After biotinylation of the λ-DNA strand, the same protocol was used to hybridise the other end as well with a complementary oligonucleotide with no biotin, complete with backbone ligation. Beads incubated at pH 7 were used for comparison, as these were found to have the greatest affinity to the colloid surface. The comparison of D and κ distributions, given in Fig. 6, reveals that there is a marked increase in diffusivity, and a decrease in confinement strength when the ssDNA ends are capped. The effect is not a total removal of the effect – dsDNA also show some stickiness to the bare beads.

4 Conclusions

We have demonstrated that colloids bind non-specifically to a λ-DNA brush and display a drastically reduced diffusivity, despite the presence of electrostatic repulsion between the negatively charged sugar–phosphate backbone of the single stranded DNA and the silica surfaces. By changing the incubation conditions of the microspheres, the hydrophobic interaction between the beads and the DNA are modified, with lower confinement and higher diffusivity for beads that are prepared and maintained at high pH, with a transition point at around pH 8. The effect of the pH is attributed to an inherent patchiness of the PEG coverage as the surface charge changes, combined with a counter-ion condensation in the Stern layer. The significance of hydrophobicity is further confirmed when the most hydrophobic element of the DNA brush, the ssDNA end of the λ-DNA is capped, further enhancing diffusivity for even the most adhesive beads.

The work presented here has important implications for the choice of protocol for the preparation of PLL–PEG coated colloids. First of all, our work shows the potential of using controlled PLL–PEG adsorption for tuning the hydrophobicity of silica colloids simply by choosing the appropriate pH during incubation. Such PLL–PEG coated silica beads are stable in solution, and easily prepared. Secondly, work study clarifies the nature of the non-specific attraction of a DNA brush to silica surfaces. Understanding such non-specific effects is important when studying the effect of *specific* interactions such as hybridization. In particular, single-stranded DNA appears to have a greater affinity for bare silica surfaces than double-stranded DNA. Furthermore, we have shown that this attraction can be modified by changing the nature of either the introduced probe

particles, the surface itself, or both. This is highly significant in the light of the phenomena highlighted in the Introduction, as they are governed just as much by diffusion dynamics as equilibrium behaviour.

Acknowledgements

We would like to thank Seth Fraden, Daan Frenkel and his team, in particular Jure Dobnikar and Tine Curk, for discussions. This project was funded by the Ernest Oppenheimer Fund (TY), the George and Lillian Schiff Foundation (TY), the Marie Curie Training Network ITN-COMPLOIDS no. 234810 (LD) and the Cavendish Laboratory (EE).

References

1 A. Saha, J. Wittmeyer and B. R. Cairns, *Nat. Rev. Mol. Cell Biol.*, 2006, **7**, 437–447.
2 K. Keren, Y. Soen, G. B. Yoseph, R. Gilad, E. Braun, U. Sivan and Y. Talmon, *Phys. Rev. Lett.*, 2002, **89**, 088103.
3 T. T. Nguyen and B. I. Shklovskii, *J. Chem. Phys.*, 2001, **115**, 7298–7308.
4 A. Meller, L. Nivon and D. Branton, *Phys. Rev. Lett.*, 2001, **86**, 3435–3438.
5 S. Ghosal, *Phys. Rev. E*, 2007, **76**, 061916.
6 M. Muthukumar, *Annu. Rev. Biophys. Biomol. Struct.*, 2007, **36**, 435–450.
7 M. Hatlo, D. Panja and R. van Roij, *Phys. Rev. Lett.*, 2011, **107**, 068101.
8 V. T. Milam, A. L. Hiddessen, J. C. Crocker, D. J. Graves and D. A. Hammer, *Langmuir*, 2003, **19**, 10317–10323.
9 N. L. Rosi and C. A. Mirkin, *Chem. Rev.*, 2005, **105**, 1547–1562.
10 M. M. Maye, D. Nykypanchuk, D. van der Lelie and O. Gang, *J. Am. Chem. Soc.*, 2006, **128**, 14020–14021.
11 T. Schmatko, B. Bozorgui, N. Geerts, D. Frenkel, E. Eiser and W. C. K. Poon, *Soft Matter*, 2007, **3**, 703–706.
12 H. Xiong, D. van der Lelie and O. Gang, *J. Am. Chem. Soc.*, 2008, **130**, 2442–2443.
13 D. Nykypanchuk, M. M. Maye, D. van der Lelie and O. Gang, *Nature*, 2008, **451**, 549–552.
14 R. Dreyfus, M. Leunissen, R. Sha, A. Tkachenko, N. Seeman, D. J. Pine and P. Chaikin, *Phys. Rev. Lett.*, 2009, **102**, 048301.
15 R. J. Macfarlane, M. R. Jones, A. J. Senesi, K. L. Young, B. Lee, J. Wu and C. A. Mirkin, *Angew. Chem., Int. Ed.*, 2010, **49**, 4589–4592.
16 C. Bustamante, J. Marko, E. Siggia and S. Smith, *Science*, 1994, **265**, 1599–1600.
17 J. Moroz and P. Nelson, *Proc. Natl. Acad. Sci. U. S. A.*, 1997, **94**, 14418–14422.
18 M.-N. Dessinges, B. Maier, Y. Zhang, M. Peliti, D. Bensimon and V. Croquette, *Phys. Rev. Lett.*, 2002, **89**, 248102.
19 J. Yan and J. Marko, *Phys. Rev. E*, 2003, **68**, 011905.
20 V. Chan, *J. Colloid Interface Sci.*, 1998, **203**, 197–207.
21 M. Y. Tolstorukov, R. L. Jernigan and V. B. Zhurkin, *J. Mol. Biol.*, 2004, **337**, 65–76.
22 X. Liu, Z. Wu, H. Nie, Z. Liu, Y. He and E. S. Yeung, *Anal. Chim. Acta*, 2007, **602**, 229–235.
23 Q. Xu, L. Feng, R. Sha, N. Seeman and P. Chaikin, *Phys. Rev. Lett.*, 2011, **106**, 228102.
24 W. Norde and A. C. Anusiem, *Colloids Surf.*, 1992, **66**, 73–80.
25 H. Tu, L. Hong, S. M. Anthony, P. V. Braun and S. Granick, *Langmuir*, 2007, **23**, 2322–2325.
26 J. Sambrook and S. Russell, *Molecular Cloning: A Laboratory Manual*, Cold Spring Harbor Laboratory Press, 3rd edn, 2001.
27 F. Sanger, *J. Mol. Biol.*, 1982, **162**, 729–773.
28 N. Geerts, S. Jahn and E. Eiser, *J. Phys.: Condens. Matter*, 2010, **22**, 104111.
29 J. Crocker and D. G. Grier, *J. Colloid Interface Sci.*, 1996, **179**, 298–310.
30 M. Abràmoff, P. Magalhães and S. Ram, *Biophotonics Intl*, 2004, **11**, 36–42.
31 O. Saengsawang, T. Remsungnen, S. Fritzsche, R. Haberlandt and S. Hannongbua, *J. Phys. Chem. B*, 2005, **109**, 5684–5890.
32 U. Wattendorf, O. Kreft, M. Textor, G. B. Sukhorukov and H. P. Merkle, *Biomacromolecules*, 2008, **9**, 100–108.
33 C. Ligoure and L. Leibler, *J. Phys.*, 1990, **51**, 1313–1328.
34 B. O'Shaughnessy and Q. Yang, *Europhys. Lett.*, 2006, **75**, 427–433.
35 C. G. Baumann, V. A. Bloomfield, S. B. Smith, C. Bustamante, M. D. Wang and S. M. Block, *Biophys. J.*, 2000, **78**, 1965–1978.
36 K. Devanand and J. C. Selser, *Macromolecules*, 1991, **24**, 5943–5947.
37 B. Lukić, S. Jeney, Z. Sviben, A. Kulik, E.-L. Florin and L. Forró, *Phys. Rev. E*, 2007, **76**, 011112.
38 T. Hiemstra, J. Dewit and W. Van Riemsdijk, *J. Colloid Interface Sci.*, 1989, **133**, 105–117.
39 S. Behrens and D. G. Grier, *Phys. Rev. E*, 2001, **64**, 050401.
40 M. Hair, *J. Non-Cryst. Solids*, 1975, **19**, 299–309.

